

SCIENTIFIC REPORTS

Correction: Retraction

OPEN

New molecular tools in *Neospora caninum* for studying apicomplexan parasite proteins

Caroline M. Mota¹, Allan L. Chen², Kevin Wang², Santhosh Nadipalam², Ajay A. Vashisht³, James A. Wohlschlegel³, Tiago W. P. Mineo¹ & Peter J. Bradley^{2,4}

The development of molecular genetics has greatly enhanced the study of the biology and pathology associated with parasites of the phylum Apicomplexa. We have established a system specifically designed for *Neospora caninum*, and used this system as a heterologous platform for the expression of foreign genes. Plasmid constructs containing fluorescent proteins or targeted genes of *Toxoplasma gondii*, driven by *N. caninum* promoters, have yielded robust expression and correct trafficking of target gene products as assessed by immunofluorescence assays and Western blot analyses. Using this approach, we here demonstrated that *N. caninum* expressing *T. gondii*'s GRA15 and ROP16 kinase are biologically active and induced immunological phenotypes consistent with *T. gondii* strains. *N. caninum* expressing TgGRA15 differentially disturbed the NF- κ B pathway, inducing an increased IL-12 production. On the other hand, *N. caninum* expressing TgROP16 induced host STAT3 phosphorylation and consequent reduction of IL-12 synthesis. These results indicate that heterologous gene expression in *N. caninum* is a useful tool for the study of specific gene functions and may allow the identification of antigenic targets responsible for the phenotypic differences observed between these two closely related apicomplexan parasites. Additionally, these observations may prove to be useful for the development of vaccine protocols to control toxoplasmosis and/or neosporosis.

Toxoplasma gondii and *Neospora caninum* are closely related coccidians that belong to a diverse group of parasitic protozoans of the phylum Apicomplexa^{1,2}. *T. gondii* is an organism that infects all warm-blooded vertebrates including humans and birds, and it is estimated that one-third of the world's population is infected by this pathogen³. On the other hand, *N. caninum* has a narrower host range, primarily targeting cattle and dogs, representing today the leading cause of bovine abortions and consequent economic losses worldwide^{1,2,4}. These parasites invade the host cells mainly through an active and complex process, induced predominantly by a series of proteins that are released from the parasite's micronemes, rhoptries and dense granules^{4,5}.

One strategy routinely used to gain better knowledge of the invasion and replication systems of these parasites is based on the development of a robust set of molecular tools that enable reliable analyses of specific protein targets⁵⁻⁷. While a wide array of tools have been developed for *T. gondii*, including an assortment of promoters, fluorescent proteins, selectable markers, and genome editing tools, few such tools are available for *N. caninum*. Developing specific tools for that genetic manipulation will certainly help understand parasite biology and host-parasite interactions and, possibly, be a part in the development of vaccine and treatment strategies against the infection by this parasite^{8,9}. In addition, the use of *N. caninum* as a heterologous system provides greater ease in molecular manipulation and the availability of advanced genetic tools allows it to serve as a model organism to study other apicomplexan parasites^{10,11}. Therefore, manipulating the pathogen genome is a way to understand the functions of specific genes in parasite development and pathogenesis.

Infections by *N. caninum* and *T. gondii* are perennial, although the correct modulation of the T helper 1 (Th1) immune responses, based on the production of interleukin-12 (IL-12) and IFN- γ , grant its hosts the ability to repress acute phase accelerated parasite replication and consequently reduce chronic phase tissue parasitism⁴.

¹Laboratory of Immunoparasitology "Dr. Mário Endsfieldz Camargo", Institute of Biomedical Sciences, Universidade Federal de Uberlândia, Uberlândia, Minas Gerais, Brazil. ²Department of Microbiology, Immunology and Molecular Genetics, University of California, Los Angeles, Los Angeles, California, USA. ³Department of Biological Chemistry and Institute of Genomics and Proteomics, University of California, Los Angeles, Los Angeles, California, USA. ⁴Molecular Biology Institute, University of California, Los Angeles, Los Angeles, California, USA. Correspondence and requests for materials should be addressed to T.W.P.M. (email: tiago.mineo@ufu.br) or P.J.B. (email: pbradley@ucla.edu)

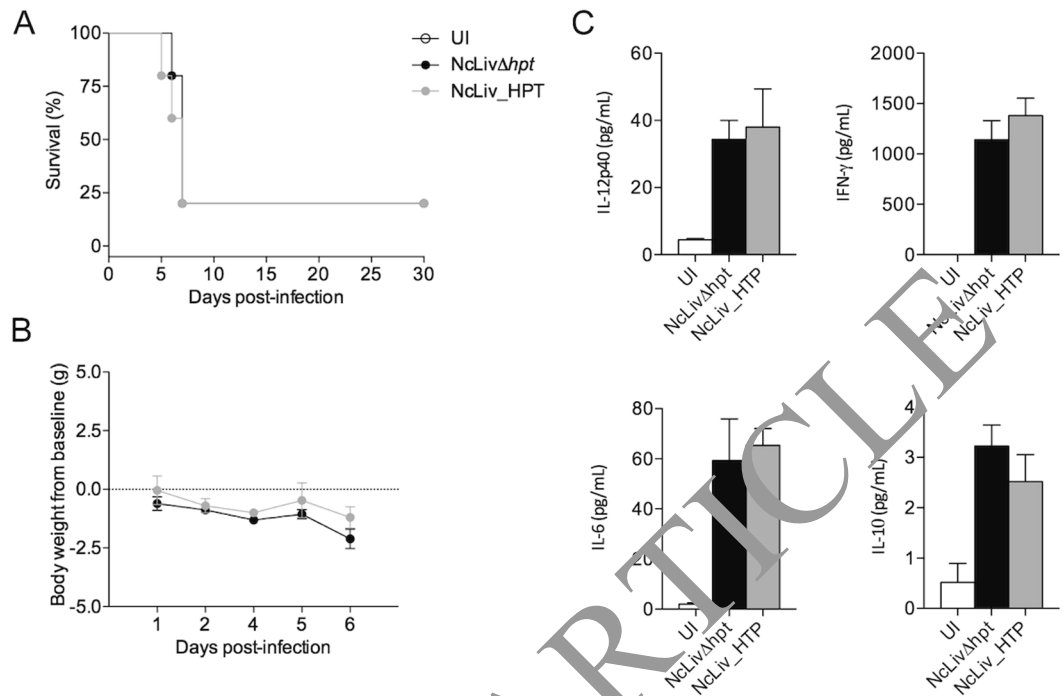


Figure 1. C57BL/6 mice infected by NcLiv Δ hpt and the complemented strain present similar virulence and cytokine profiles *in vivo*. C57BL/6 mice were infected with 1×10^6 tachyzoites of NcLiv Δ hpt and NcLiv_HPT for 3 days for cytokine measurement or 30 days for survival analysis. As negative controls, mice were inoculated with PBS (uninfected - UI). (A) Survival curves and (B) Body weight from baseline of C57BL/6 mice after infection with *N. caninum*, (C) Cytokine production in the peritoneal wash (6 mice/group) after 3 days of infection measured by CBA. Values are representative of two independent experiments, indicating mean \pm SEM of cytokine levels in relation the standard curve ($P < 0.05$; ANOVA and Bonferroni multiple comparison post-test).

¹² The dense granule (GRA) and rhoptry (ROP) proteins have been well described to induce a direct impact on signaling pathways of the host's immune system. Previous analyses have shown that key parasite effector proteins are injected into macrophages and activate signaling pathways that regulate inflammation. The *Toxoplasma* rhoptry 16 kinase (ROP16) secreted protein into the host cytosol, induces a direct and sustained phosphorylation of signal transducer and activator of transcription 3 (STAT3) and STAT6, leading to altered cytokine profiles and repression of interleukin 12 signaling in type I/III strains. In contrast, *T. gondii* type II strains encode an isoform of the dense granule protein 15 (GRA15), that activates the NF- κ B pathway, leading to increased IL-12 production^{13–16}.

Therefore, in order to use *Neospora* as a template model for the better understanding of *T. gondii* genes, we describe here the development of a specific heterologous expression system that promises to be a useful tool for the identification and characterization of genes involved in the pathogenesis associated with toxoplasmosis, and that may also be used to develop a safe vaccine to control toxoplasmosis and/or neosporosis.

Results

HXGPRT gene deletion does not alter infection phenotype and immune responses. To aid in the genetic manipulation of *N. caninum*, we first sought to disrupt the selectable marker HXGPRT by homologous recombination. We amplified the genomic HXGPRT locus including 1.3 kb upstream and downstream of the gene and then created a HXGPRT knockout plasmid by deleting exons 2–4. This plasmid was linearized, transfected into wild-type NcLiv parasites, and Δ hxgp r t parasites were selected with 6-thioxanthine and cloned by limiting dilution¹⁷. A knockout clone was chosen that failed to grow in positive selection and the absence of the deleted region was confirmed by PCR (not shown).

To assess whether the depletion of the HXGPRT gene could lead to a defect in virulence or altered immune response induced by the parasite, we initially complemented HXGPRT in the NcLiv knockout parasites (NcLiv Δ hpt) by homologous recombination. The HXGPRT-complemented parasites (NcLiv_HPT) were selected with mycophenolic acid plus xanthine and cloned by limiting dilution. In the next step, C57BL/6 mice were infected with NcLiv knockout for HXGPRT gene (NcLiv Δ hpt) and HXGPRT complemented parasites (NcLiv_HPT). All mice injected intraperitoneally (i.p.) with 1×10^6 NcLiv Δ hpt or NcLiv_HPT tachyzoites presented similar survival and weight loss patterns, along with unaltered cytokine profiles (Fig. 1A–C). This data confirmed our hypothesis that deletion of HXGPRT does not affect the parasite virulence and consequent elicited immune responses.

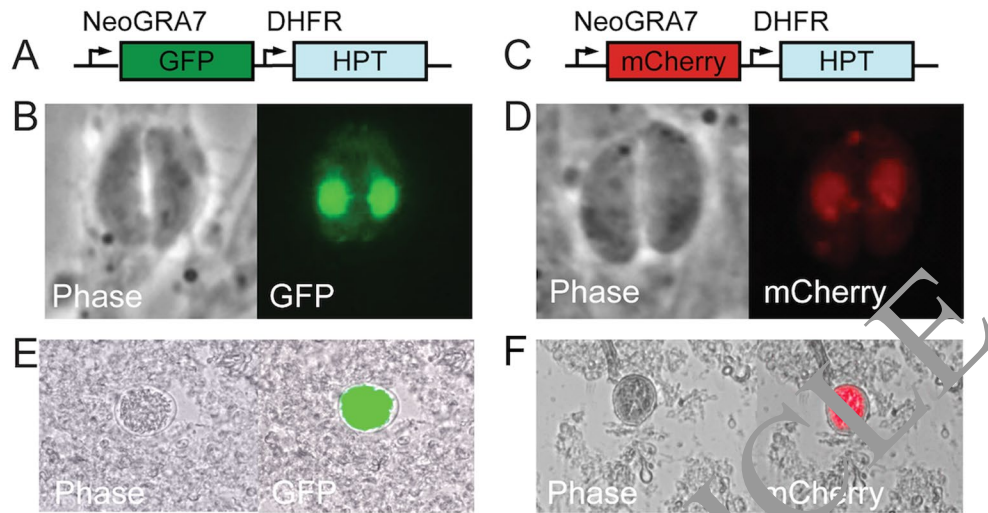


Figure 2. Stable expression of GFP and mCherry in tachyzoites and tissue cysts of *N. caninum*. (A) Diagram of the expression cassette encoding GFP, driven by the *N. caninum* GRA7 promoter, (B) GFP-expressing *N. caninum* tachyzoites, microscope magnification: 63x, (C) diagram of the expression cassette encoding mCherry, driven by the *N. caninum* GRA7 promoter, (D) mCherry-expressing *N. caninum* tachyzoites, microscope magnification: 63x, (E) tissue cyst found in the brain of mice infected for 30 days with GFP-expressing *N. caninum*, microscope magnification: 40x, (F) tissue cyst found in the brain of mice infected for 30 days with mCherry-expressing *N. caninum*, microscope magnification: 40x.

Identification of GRA7 and ROP13 as efficient promoters for the expression of heterologous proteins in *N. caninum*.

In *T. gondii*, cell cycle transcriptional profile analyses have revealed two major groups of expressed genes; one which is constitutive throughout the cell cycle and a second whose expression cycles are coincident with the production of new cellular components of daughter cells (e.g. the secretory micronemes and rhoptries). To engineer expression systems for both types of proteins in *N. caninum*, we chose to utilize the GRA7 promoter that would be expected to provide strong constitutive expression, as well as ROP13 that would be more appropriate for expression of cell cycle regulated genes. We initially tested the expression from these promoters using GFP or mCherry as targets. NcLiv Δ hpt tachyzoites were transfected with pGRA7-GFP/mCherry-HPT or pROP13-GFP/mCherry-HPT constructs and grown in medium containing mycophenolic acid plus xanthine. The selection produced stable populations, which exhibited a high frequency of transformed parasites that were identified by brightly fluorescent tachyzoites. We also observed robust expression of the fluorescent proteins in tissue cysts isolated from the brains of infected animals (Fig. 2A–F), which helped the estimation of chronic phase parasite burden in infected mice – approximately 100 cysts/mice. These stably expressing lines demonstrate the effectiveness of the *Neospora* promoters and additionally provide valuable tools for parasite load determination.

Heterologous expression of *T. gondii* virulence factors in *N. caninum*.

To assess whether *N. caninum* would be a suitable model for heterologous expression of apicomplexan host modulatory factors, we generated expression cassettes that included a C-terminal hemagglutinin (HA) tag, driven by the GRA7 or ROP13 promoters (Figs 3A and 4A). We then engineered constructs for expression of the *T. gondii* virulence factors GRA15 (TGME49_275470, driven by the GRA7 promoter) and ROP16 (TGGT1_262730, driven by the ROP13 promoter) in NcLiv Δ hpt tachyzoites. The constructs were transfected into *Neospora* and localization of the tagged proteins was assessed by immunofluorescence assay (IFA) and western blotting (WB). As expected, IFA showed that the tagged GRA15 constructs were correctly targeted to the dense granules and into the PV (Fig. 3B) and ROP16 was correctly targeted to the parasites' rhoptries (Fig. 4B). These localizations were confirmed by co-localization with cross-reactive *Toxoplasma* anti-GRA14¹⁸ and anti-ROP13¹⁹ antisera, respectively. The proteins additionally migrated at their expected size by Western blot of whole parasite lysates, which showed no signal from control NcLiv Δ hpt parasites (Figs 3C and 4C). An attempt of heterologous expression of GRA15 was performed using the pTgGRA1-HA-HPT plasmid designed for *T. gondii*. Although we did not quantify differences, lower expression levels of GRA15 were observed when the *T. gondii* vector was used, if compared to those transfected with *N. caninum* specific promoter. Collectively, these data indicate that the GRA15 and ROP16 proteins expressed in *N. caninum* were correctly processed and targeted.

Expression of the selected heterologous *Toxoplasma* proteins does not alter *N. caninum* tachyzoite fitness.

To assess the growth of knock-in parasites, a competition assay was performed between the modified parasites and the parental line (NcLiv Δ hpt). Both parental and NcLiv_GRA15 or NcLiv_ROP16 parasites were mixed in a 1:1 ratio and allowed to grow in human fibroblast monolayers (Figs 5A and 6A). Based on the results of these experiments, we observed that the addition of these genes did not compromise the growth ratio of the tachyzoites. Additionally, we performed a plaque assay to examine the lytic cycle (invasion, replication,

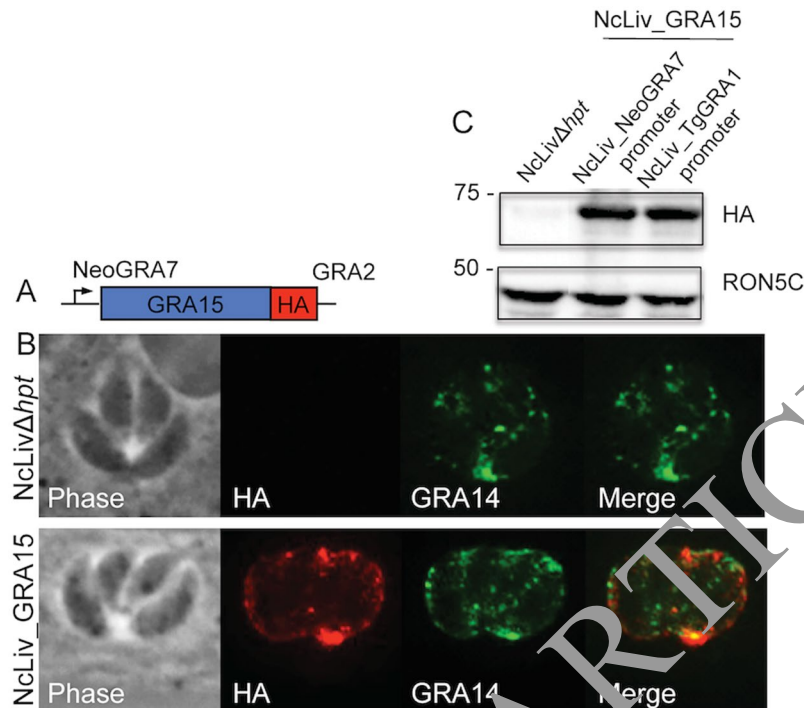


Figure 3. Expression of type II *T. gondii* GRA15 gene in *N. caninum*. (A) Diagram of the expression cassette encoding TgGRA15 plus C-terminal 3xHA epitope tag, driven by the *N. caninum* GRA7 promoter, (B) expression of GRA15-expressing *N. caninum* tachyzoites confirmed by IFA. GRA15 was localized in the parasitophorous vacuole by its HA tag, where it colocalized with the GRA14 marker. Red, rabbit anti-HA antibody; green, mouse anti-GRA14 antibody. Microscope magnification, 63x, (C) Expression of TgGRA15 in transgenic *N. caninum* tachyzoites confirmed by Western blot. TgGRA15 was detected by its HA tag present in the constructs driven by *N. caninum* GRA7 promoter. Full-length blots are available in Supplementary dataset file.

and egress) over an extended time period (8 days). The yielded results of these assays was that NcLiv_GRA15 or NcLiv_ROP16 plaques were not significantly altered in size and number compared to the parental lines (Figs 5B and 6B). Altogether, these results indicate that the insertion of heterologous genes in *N. caninum* through the designed vectors did not alter parasite fitness.

***N. caninum* tachyzoites expressing heterologous genes mimic *T. gondii*-induced biological phenotypes.**

The next step was to determine whether the expression of known *T. gondii* immunomodulatory genes would induce compatible biological phenomena in transgenic *N. caninum* tachyzoites. We first generated a construct containing GRA15 fused to BirA* with a C-terminal hemagglutinin (HA) tag, driven from the *N. caninum* GRA7 promoter (Fig. 7A). The GRA15-BirA* fusion was integrated into the genome of NcLivΔhpt parasites and its localization was assessed by immunofluorescence assay (IFA). As expected, we observed staining in the parasitophorous vacuole (Fig. 7B), a pattern consistent with dense granule proteins. To determine which proximal proteins in the parasitophorous vacuole were labeled by the GRA15-BirA*+ *N. caninum* tachyzoites, we grew parasites in medium supplemented with biotin and stained for biotinylated proteins using fluorophore-conjugated streptavidin. Although parental *N. caninum* parasites have endogenously biotinylated proteins in the apicoplast that are labeled by streptavidin (Fig. 7B, top)²⁰, GRA15-BirA*+ *N. caninum* tachyzoites showed a robust streptavidin staining in the parasitophorous vacuole, indicating that the biotin ligase fusion was active and that it labeled proteins in the parasitophorous vacuole (Fig. 7B, bottom). After verification that GRA15-BirA*+ parasites labeled varied cellular proteins by Western blotting using a streptavidin-horseradish peroxidase (HRP) probe (Fig. 7C), we identified the labeled host targets by affinity purification of the biotinylated proteins and subsequent analysis by mass spectrometry (full list of hits in Table S2). Among the differential GRA15-BirA*+ host targets, we clearly identified an enrichment in the members of the NF-κB family and related pathways (Fig. 7D), attuned with previous descriptions of the molecular mechanisms involving GRA15^{15, 16}. We then assessed whether the activation of the NF-κB pathway by the *N. caninum* GRA15-BirA*+ tachyzoites would also compromise the production of IL-12p40 by infected macrophages. Infection of bone marrow derived macrophages (BMDMs) with live parental (NcLivΔhpt) and transgenic (NcLiv_GRA15) tachyzoites revealed a pronounced increase in IL-12p40 production in cells infected with NcLiv_GRA15 (Fig. 7E), again corroborating with the data available in the literature^{15, 16}.

We additionally assessed whether the expression of ROP16 in *N. caninum* would also simulate the modulatory effects in immune responses induced by type I *T. gondii* tachyzoites. We first checked for the presence of STAT3 phosphorylation in the host cells. We analyzed infected fibroblasts with the parental line and NcLiv_ROP16 parasites with antibodies specific for the tyrosine-phosphorylated (activated) forms of STAT3 using IFA and WB. Both

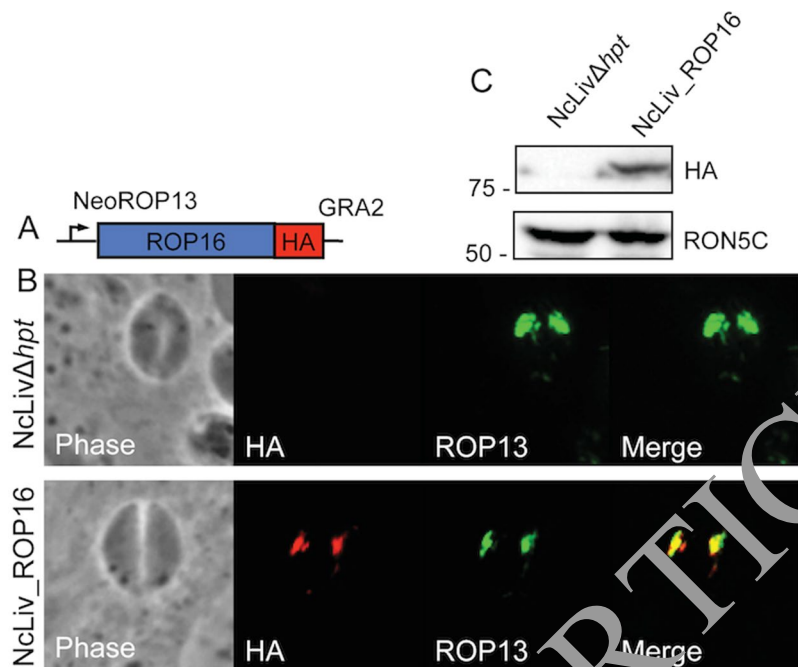


Figure 4. Expression of type I *T. gondii* ROP16 gene in *N. caninum*. **(A)** Diagram of the expression cassette encoding TgROP16 plus C-terminal 3xHA epitope tag, driven by the *N. caninum* ROP13 promoter, **(B)** expression of ROP16-expressing *N. caninum* tachyzoites confirmed by IFA. ROP16 was localized at the rhoptries by its HA tag, which colocalized with ROP13 marker. Red, rabbit anti-HA antibody; green, mouse anti-ROP13 antibody. Microscope magnification: 63x, **(C)** Expression of TgROP16 in transgenic *N. caninum* tachyzoites confirmed by Western blot. TgROP16 was detected by its HA tag present in the constructs driven by *N. caninum* ROP13 promoter. Full-length blots are available in Supplementary dataset file.

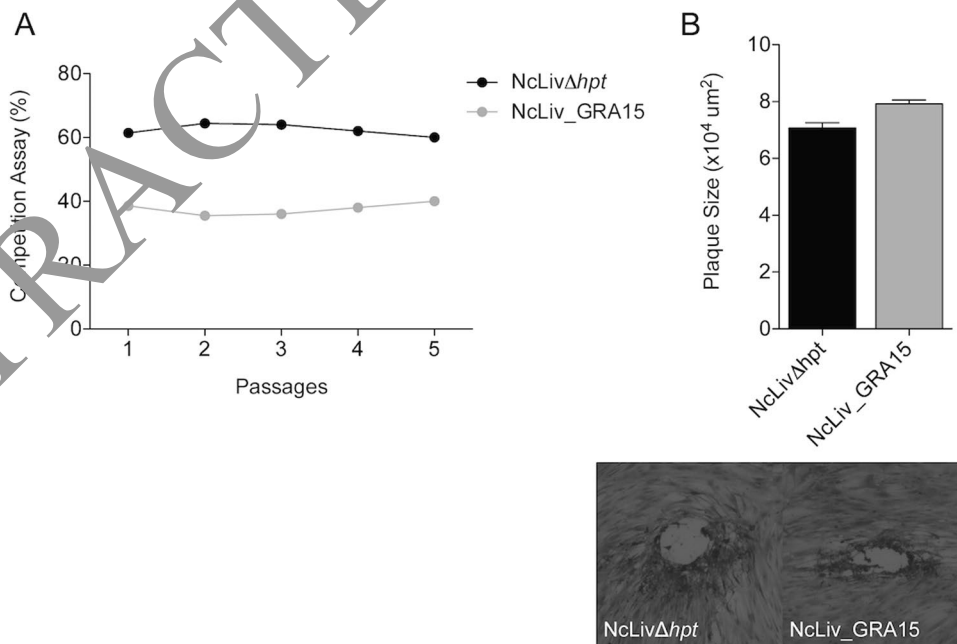


Figure 5. GRA15 expression in *N. caninum* does not compromise parasite fitness. **(A)** Growth competition assay of parental (NcLiv Δ hpt) and NcLiv_GRA15 strains, co-cultured for 6 passages (50%/50% proportion), **(B)** plaque formation of parental (NcLiv Δ hpt) and NcLiv_GRA15 strains, based on multiple lytic cycles. The area of each plaque was determined at 8 days post infection. Values are representative of two independent experiments indicating mean \pm SEM of plaque size (* $P < 0.05$; Student's t-test).

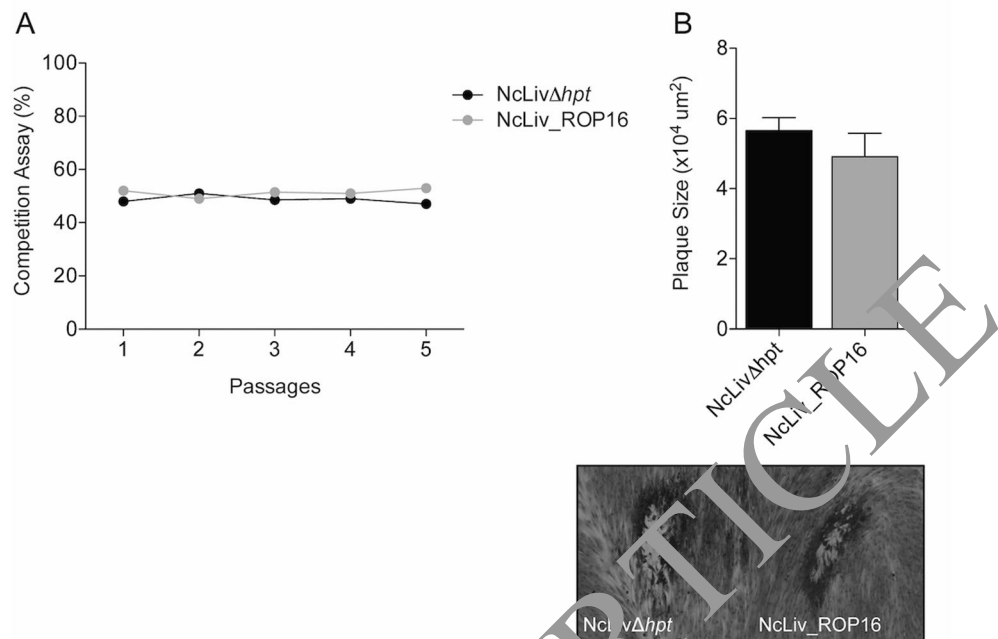


Figure 6. ROP16 expression in *N. caninum* does not compromise parasite fitness. **(A)** Growth competition assay of parental (NcLiv Δ hpt) and NcLiv_ROP16 strains co-cultured for 6 passages (80%/20% and 50%/50% proportions), **(B)** plaque formation of parental (NcLiv Δ hpt) and NcLiv_ROP16 strains, based on multiple lytic cycles. The area of each plaque was determined at 3 days post infection. Values are representative of two independent experiments indicating mean \pm SEM of plaque size (* $P < 0.05$; Student's t-test).

methods revealed that, after 1 day of infection, serum-starved HFFs infected with RH Δ hpt and NcLiv_ROP16 induced activation of STAT3, while STAT3 phosphorylation was absent in cells infected by NcLiv Δ hpt parasites (Fig. 8A and B).

Given that the primary biological feature of ROP16 kinase was preserved in transgenic *N. caninum* tachyzoites, we then aimed to assess whether the activation of the STAT3 pathway would compromise the production of IL-12p40 by infected macrophages. After infection of BMDMs with live parental and transgenic parasites, we observed that NcLiv_ROP16 tachyzoites induced significantly lower levels of IL-12p40, compared to BMDMs infected with NcLiv Δ hpt. Additionally, in order to eliminate possible caveats regarding bone marrow differentiation, we ran the same experimental layout with naive spleen cells and, again, we observed a pronounced decrease in IL-12p40 production in cells infected with NcLiv_ROP16 (Fig. 8C). Together, this result demonstrates that the biological phenotypes induced by the heterologous proteins expressed in *N. caninum* have been preserved. Therefore, *Neospora* can be used as a platform for the study of possible virulence factors of Apicomplexa parasites.

Discussion

Neospora caninum is a coccidian parasite, closely related to *Toxoplasma gondii*, with broad host range and worldwide distribution, causing neuromuscular disease in dogs and abortion or reproductive disorders in cattle, representing significant economic losses worldwide^{1,21}. The use of *N. caninum* as a heterologous platform for the expression of *T. gondii* genes has been explored here, and we show that this system is likely to be useful for the identification and characterization of modulatory factors involved in the pathogenesis of these two related parasites. Additionally, this system has to be considered as a possible live vaccine vector, due to its potential of delivering *T. gondii* virulence factors in an avirulent parasite to most animal species.

We have provided in the present study a simple and reliable technique to stably express *T. gondii* proteins in *N. caninum*. Few research groups have attempted to genetically manipulate *N. caninum* tachyzoites, and most used methods that rely on vectors originally designed for *T. gondii*^{10, 11, 22–24}. While these vectors have been successful at expressing foreign genes in *N. caninum*, we and others have noticed that expression from *Toxoplasma* promoters in *Neospora* (particularly for genes encoding rhoptry proteins) often results in varying expression levels, indicating expression of transgenes would best be suited using endogenous *N. caninum* promoters^{25, 26}. We present here molecular advances that are based on a system specifically designed for *N. caninum*, which was able to express the targeted heterologous genes with high efficiency. Thus, this method has enhanced our ability to manipulate the *N. caninum* genome and will enable high-throughput intervention in a broad range of genetic loci. It's noteworthy that the genetic manipulation of the parasites did not affect tachyzoite fitness. The growth ratio of NcLiv Δ hpt was similar to the NcLiv wild type strain *in vitro*, and, according to *in vivo* experiments performed in our lab, the parasites' lethal doses were unchanged.

The first step to obtain transgenic *N. caninum* expressing foreign proteins was the development of parasites deleted for the hypoxanthine-xanthine-guanine phosphoribosyltransferase (HXGPRT) selectable marker¹⁷.

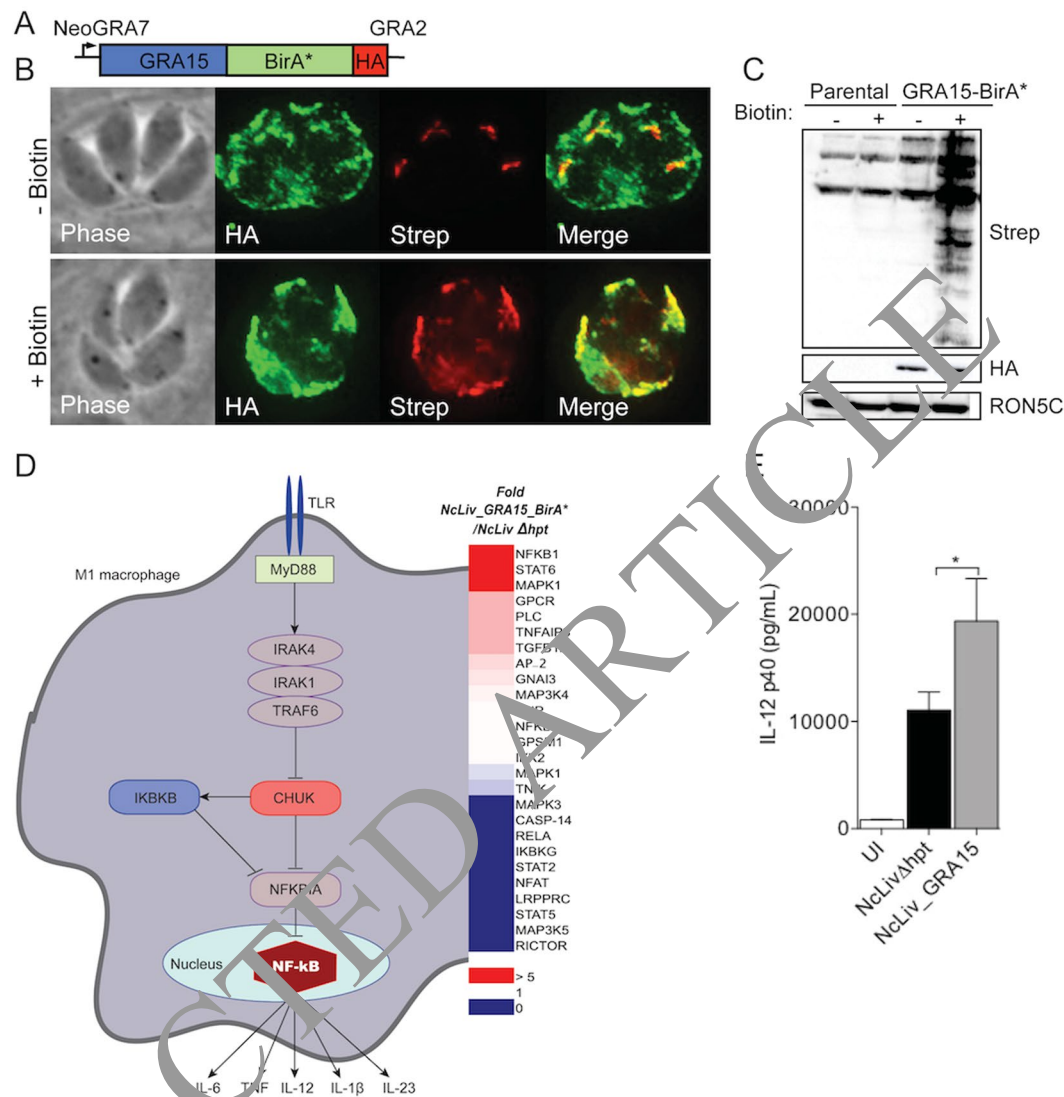


Figure 7. GRA15 expression in *N. caninum* upregulates the NF- κ B pathway members and increases IL-12p40 production. **(A)** Diagram of the expression cassette encoding GRA15 fused to BirA*, plus a C-terminal 3xHA epitope, driven by the GRA7 promoter, **(B)** IFA of GRA15-BirA*-expressing parasites, grown for 48 h with or without biotin. GRA15-BirA* localizes to the parasite dense granules and biotinylates proteins in a biotin-dependent manner. Endogenously biotinylated proteins in the apicoplast are detectable, even in the absence of biotin. Bottom panel, Green, mouse anti-HA antibody; red, streptavidin-Alexa 594. Microscope magnification: 63x, **(C)** Western blot comparing the profile of biotinylated proteins from lysates cells infected with parental and GRA15-BirA* parasites, **(D)** Diagram and heat map of the mass spectrometry results of the biotinylated proteins analyzed by the Pathway Studio software shows the upregulation of the NF- κ B pathway, **(E)** NcLiv_GRA15 induces the upregulation of IL-12p40 in macrophages. Values are representative of two independent experiments indicating mean \pm SEM of cytokine levels in relation the standard curve (* $P < 0.05$; ANOVA and Bonferroni multiple comparison post-test). Full-length blots are available in Supplementary dataset file.

Neospora tachyzoites deficient in HXGPRT activity can be negatively selected in the presence of 6-thioxanthine (6-TX), whereas strains expressing HXGPRT activity can be selected with mycophenolic acid and xanthine (MX) positive selection. This strain will be useful for expression of transgenes in *Neospora*, and will also be useful as a selectable marker for knockouts via homologous recombination or CRISPR.

Previous groups have attempted to engineer *N. caninum* tachyzoites resistant to different drugs. Pyrimethamine-resistant *N. caninum* was generated through the incorporation of dihydrofolate reductase-thymidylate synthase (DHFR-TS) and used to stably express the *T. gondii* Type I ROP18²² and Lac-Z²⁵. The chloramphenicol acetyltransferase (CAT) resistance was also previously used for the expression of the Lac-Z in *N. caninum*²⁶. We proposed, therefore, to develop a modified NcLiv strain of *N. caninum* deficient in HXGPRT, which facilitates the consequent genome editing and does not alter growth and the cytokine profile, nor needs

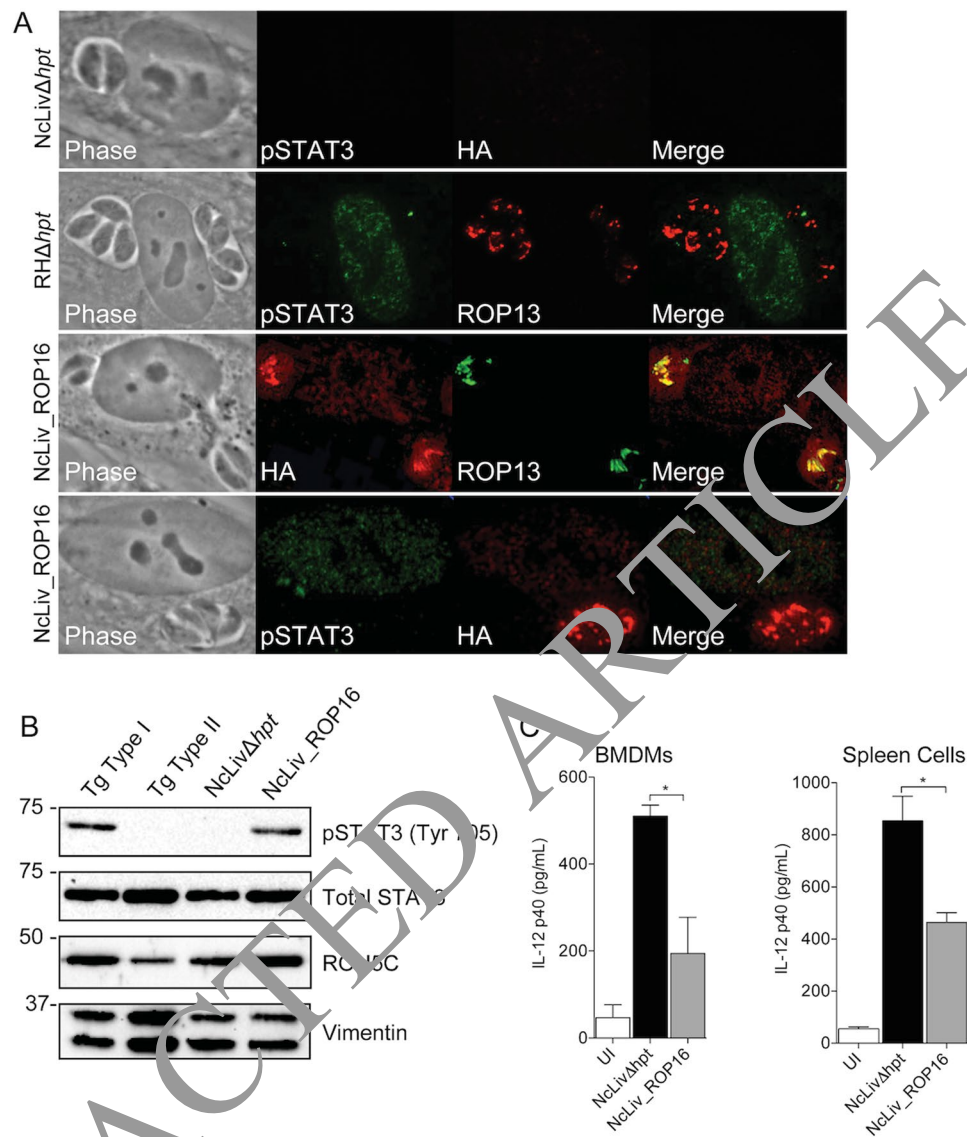


Figure 8. ROP16 expression induces STAT3 phosphorylation and down-modulation of IL-12p40 production. **(A)** Immunofluorescence analysis of ROP16-dependent activation of STAT3. HFFs were infected with type I *T. gondii* (RH Δ hpt), NcLiv Δ hpt or NcLiv_ROP16 (MOI 10) for 18 h, fixed and incubated with antibodies against parasite HA tag, Rop13 or the phosphorylated forms of STAT3 (Tyr 705). Microscope magnification: 63x. **(B)** Western blot analysis of ROP16-dependent phosphorylation of STAT3. Serum-starved HFFs were infected with a type I and type II strains of *T. gondii*, NcLiv Δ hpt or NcLiv_ROP16 and 18 h after infection, cells were lysed and analysed by immunoblotting. Virmetin (host cell-specific) and RON5C (parasite-specific) levels are shown as loading controls, **(C)** NcLiv_ROP16 inhibits IL-12p40 in infected macrophages and spleen cells. Values are representative of two independent experiments indicating mean \pm SEM of cytokine levels in relation the standard curve (* $P < 0.05$; ANOVA and Bonferroni multiple comparison post-test). Full-length blots are available in Supplementary dataset file.

constant drug pressure for selection, which may be used as a parental strain when tested in parallel with *N. caninum* expressing foreign proteins.

We also determined specific *N. caninum* promoters (ROP13: NCLIV_055850; GRA7: NCLIV_021640) that correctly and abundantly express genes associated with both constitutive and cyclical cell cycle expression profiles, which provides a more stable and efficient protocol during the desired genetic manipulation in NcLiv Δ hpt strains. The expression of gene targets through both promoters induced a higher number of positive populations, simplifying the process of obtaining positive clones from the transfected populations. Additionally, the generation of *N. caninum* tachyzoites expressing mCherry and GFP - driven by those promoters - are relevant tools to quantify and detect parasite burden. Those strains can be used in experiments that rely on microscopy and flow cytometry, during *in vitro* and *in vivo* assays, to detect and phenotype parasite-harboring cells or tissue cysts. To date, the detection and quantification of *N. caninum* required parasite-specific antibodies, fluorescent probes²⁷, genomic DNA quantification²⁷ or, recently, by using transgenic parasites expressing Lac-Z²⁶. All of these methods

present its caveats, and are certainly more time-consuming, in addition of being restricted to the acute infection during *in vivo* protocols.

Targeted genetic manipulation has been the method of choice for functional genomic analysis, in order to obtain a detailed view of gene functions and induced phenotype(s). *Toxoplasma* proteins have been unveiled as key elements underlying the unique intricate relationships of these parasites with their hosts. A set of microbial products has been already characterized as potent hijackers of host cell cellular properties and functions to the advantage of the microbe^{5, 8, 28}. Many of these are rhostry proteins (i.e. ROP16, ROP18 and ROP5) that are secreted into the host cell cytoplasm at the onset of cell invasion to subvert host signaling pathways and defense systems^{8, 13, 22, 29}. In addition, the dense granule proteins are secreted once parasites reside within the parasitophorous vacuole (PV) and are detected in the PV space and at the PV membrane (PVM). Since the 1990s, their functions were described to be restricted to the PV maturation, efficiently providing the requirements for parasite growth³⁰. Research in the area has significantly increased since the beginning of the decade, especially due to the effects described for different dense granule proteins that were shown to directly or indirectly manipulate the host's pathways, being also implicated in mechanisms the pathogenesis of the infection^{15, 16, 20}.

GRA15 and ROP16 have been described as major virulence factors whose activity underlies the differences in the pathogenesis observed between distinct *T. gondii* strains^{13–16}. Previous studies demonstrated that those parasite effector proteins are injected into the host cell cytoplasm, modulating specific signaling pathways that regulate the inflammatory process. *In vitro* studies determined that type I and III ROP16, but not type II, induced sustained phosphorylation of STAT3 and STAT6 and this was genetically linked to the level of IL-12 synthesis, which is central to the host response to resist against *T. gondii* infection^{13–15, 31, 32}. In contrast, the type II strains, but not the type I/III strains, encodes a version of the protein GRA15, which activates the transcription factor NF- κ B pathway that is composed of five members: p50 (NF- κ B1), p52 (NF- κ B2), p65 (RelA), RelB, and c-Rel¹⁶. GRA15, in an opposite manner to ROP16, induces the production of pro-inflammatory mediators through this activation pathway, as IL-12p40^{13–15}.

Based on this rationale, we developed *N. caninum* expressing *T. gondii* proteins with well characterized biological effect (ROP16 and GRA15), in order to assess whether our expression model was working properly. After checking that the heterologous proteins were correctly targeted, we verified that there was no clear distinction in the phenotype of the mutants regarding the invasion process and its lytic cycles, if compared to the parental line, and that the recombinant strains were stable after several passages *in vitro* and *in vivo* without drug selection. Functionally, as expected, we found that *N. caninum* expressing GRA15 positively modulated some members of NF- κ B family, with emphasis to NF- κ B1, increasing IL-12p40 production in macrophages. Furthermore, the transgenic strain expressing ROP16 induced STAT3 phosphorylation, differently from the parental line, phenomenon that was associated with the reduction of IL-12 production by macrophages and spleen cells.

In conclusion, molecular genetics provides powerful investigative approaches that can greatly improve our understanding of intracellular pathogens and their interactions with host cells. This study indicates that the vectors here developed for manipulation of *N. caninum* parasite increase the efficiency with which these molecular manipulations can be performed and that it can be directly applicable for a safe and stable transformation of *N. caninum*. The development of molecular genetics for *N. caninum* will certainly enhance knowledge of neosporosis and, indirectly, may be used as a heterologous expression system to unravel the processing, targeting, and function of *T. gondii* proteins.

Methods

Ethics Statement. All animal studies were approved by the animal research committee at UFU (Comitê de Ética na Utilização de Animais da Universidade Federal de Uberlândia – CEUA/UFU), under protocol number 09/16. All procedures including housing and welfare were carried out in accordance with the recommendations in the Guiding Principles for Biomedical Research Involving Animals of the International Council for Laboratory Animal Science (ICLAS), countersigned by the Conselho Nacional de Controle de Experimentação Animal (CONCEA; Brazilian National Consul for the Control of Animal Experimentation) in its E-book (http://www.mct.gov.br/upd_blob/0238/238271.pdf). The UFU animal facility (Centro de Bioterismo e Experimentação Animal - CBEA/UFU) is accredited by the CONCEA (CIAEP: 01.0105.2014) and Comissão Técnica Nacional de Biossegurança (CTNBio, Brazilian National Commission on Biossecurity; CQB: 163/02).

Animals. Female C57BL/6 mice, 6–8 weeks old, were bred and maintained in small groups inside isolator cages, with light/dark cycle of 12 hours, with food and water *ad libitum*. All mice were obtained and maintained at CBEA/UFU.

Host cells and parasite culture. Parental NcLiv Δ *hpt* and modified strains of *N. caninum* were maintained by serial passages in confluent monolayers of human foreskin fibroblast (HFF) cells, cultured in complete Dulbecco's Modified Eagle's Medium supplemented with 2 mM glutamine, 100 U/mL penicillin and 100 μ g/mL streptomycin, at 37 °C in 5% CO₂ atmosphere. Parasite suspensions were obtained as previously described¹⁹.

Primers. All oligonucleotide primers used in the development of plasmids for *HXGPRT* disruption and Neospora expression constructs are listed in Table S1.

***HXGPRT* gene disruption and complementation.** For disruption of *HXGPRT* in *N. caninum*, the *HXGPRT* locus was amplified using primers P1 and P2 and cloned into the TOPO-XL vector (P1/P2; Table S1). Exons 2–4 were deleted using endogenous Sall sites and recircularization. The plasmid was linearized and transfected into wild-type NcLiv parasites. The selections for *HXGPRT*-deficient parasites were carried out using 80 μ g/mL 6-TX for 4 weeks after which the parasites were cloned by limiting dilution. Disruption of *HXGPRT* was confirmed by PCR and failure of the strain to grow in 25 μ g/mL mycophenolic acid plus 25 μ g/mL xanthine

(MPA/X). For *HXGPRT* complementation, after *HXGPRT* amplification in subcloning into the pJET vector, the plasmid was linearized by Eco-RV restriction digest and 100 µg of DNA transfected by electroporation into *NcLivΔhpt* parasites. The transfected parasites were grown in MPA/X media and the selected parasites were cloned by limiting dilution in 96 well plates.

Generation of the GFP- and mCherry-expressing *NcLivΔhpt* parasite. The GFP (P3/P4; Table S1) and mCherry (P5/P6; Table S1) coding sequences were PCR amplified using the designated primers. The resulting PCR product was cloned in a pJET vector. The insert was cleaved with Nsi I and Pac I and expressed in pNeoGRA7 (NCLIV_021640) and pNeoROP13 (NCLIV_055850) plasmids (Fig. 2). Stable transformants were selected using medium containing 25 µg/mL mycophenolic acid plus 25 µg/mL xanthine (for *HXGPRT* plasmids) and cloned by limited dilution in 96 well plates. To confirm proper GFP and mCherry expression, transgenic tachyzoites were analyzed by IFA and WB. To assess the fluorescent cysts, mice were infected for 30 days and the brain was collected and homogenized for the screening. The cysts were visualized and photographed with an inverted fluorescent microscope (EVOSfl, Thermo Scientific).

Generation of the GRA15 and ROP16 knock-in parasites. Targeting constructs were engineered using the pNeoGRA7-HA-HPT or pNeoROP13-HA-HPT or pTgGRA1-HA-HPT vector. Briefly, Type II GRA15 (P7/P8; Table S1) and Type I ROP16 (P9/P10; Table S1) of *T. gondii* gene locus are defined by TGME49_275470 and TGGT1_262730 in the current *T. gondii* genome database (www.toxodb.org; version 6.0). The genes were cloned by PCR with engineered NsiI and NotI sites. After amplification in a pJET vector, the GRA15 and ROP16 inserts were fused in frame with a plasmid using the same restriction sites (Figs 3 and 4). The constructs were linearized by HindIII and 75 µg of the resulting DNA were transfected by electroporation into *NcLivΔhpt* parasites. Stable transformants were selected using medium containing 25 µg/mL mycophenolic acid plus 25 µg/mL xanthine and cloned by limited dilution in 96 well plates. To confirm proper GRA15 and ROP16 targeting and expression, transgenic parasites were analyzed by IFA and WB.

To generate the GRA15-BirA* fusion, the BirA* was inserted into pGRA7-HA-HPT in frame, between the 3' end of GRA15 and the HA epitope tag, to generate the construct pGRA7-GRA15-BirA*-HA-HPT. One hundred micrograms of the construct was linearized with HindIII and transfected into *NcLivΔhpt* parasites. The parasites were selected with medium containing 25 µg/mL mycophenolic acid-xanthine, cloned by limiting dilution, and screened by IFA and WB for the HA tag. A clone expressing the correct fusion protein was selected.

Immunofluorescence assay and fluorescence microscopy. For IFAs, wild type and transgenic *N. caninum* strains were used to infect coverslips of HFFs for 24 hours. The coverslips were then fixed in 3.7% formaldehyde/PBS for 15 minutes. The coverslips were washed in phosphate-buffered saline (PBS) and blocked and permeabilized in a solution containing PBS/3% bovine serum albumin (BSA)/0.2% Triton X-100 for 30 minutes. Samples were then incubated with primary antibody diluted in PBS, along with BSA (3%) and Triton X-100 (0.2%) for 1 hour. The samples were then washed in PBS and treated with species-specific secondary antibodies conjugated to Alexa 594/488, diluted 1:2000 in PBS + BSA (3%). Following a new washing cycle, coverslips were mounted onto microscope slides with Vectashield mounting media and the fluorescence was observed using a Zeiss Axio Imager Z1 microscope.

Western Blot analysis. Parental and modified strains whole-parasite lysates were separated by 12% SDS-PAGE. Samples were transferred to nitrocellulose overnight and probed with primary antibodies. For all secondary antibody incubations, horseradish peroxidase (HRP)-conjugated goat anti-mouse or goat anti-rabbit antibodies were used at a 1:2000 dilution. Following secondary incubation, a chemiluminescent substrate was used for the detection of HRP activity.

Affinity capture of biotinylated proteins. HFF monolayers infected with parasites expressing BirA* fusions, or the respective parental line, were grown in medium containing 150 µM biotin for 48 h prior to parasite egress^{20,33}. Infected cells were then collected, washed in PBS, and lysed in RIPA buffer (50 mM Tris [pH 7.5], 150 mM NaCl, 0.1% SDS, 0.5% sodium deoxycholate, 1% NP-40) supplemented with Complete protease inhibitor cocktail (Roche) for 30 min on ice. Lysates were centrifuged for 15 min at 14,000 × g to pellet insoluble debris and then incubated with PureProteome streptavidin magnetic beads at room temperature, for 4 h, under gentle agitation. Beads were collected using magnets and washed five times in RIPA buffer, followed by three washes in 8 M urea buffer (50 mM Tris-HCl [pH 7.4], 150 mM NaCl). Ten percent of each sample was boiled in Laemmli sample buffer, and eluted proteins were analyzed by Western blotting by streptavidin-HRP prior to mass spectrometry.

Mass spectrometry of biotinylated proteins. Purified proteins bound to streptavidin beads were reduced, alkylated, and digested by sequential addition of Lys-C and trypsin proteases^{33,34}. The peptide mixture was desalted using C₁₈ tips and fractionated online using a 75 µM inner diameter fritted fused silica capillary column with a 5 µM pulled electrospray tip, and packed in house with 15 cm of Luna C₁₈ 3 µM reversed-phase particles. The gradient was delivered by an easy-nLC 1000 ultrahigh-pressure liquid chromatography (UHPLC) system (Thermo Scientific). Tandem mass spectrometry (MS/MS) spectra were collected on a Q-Exactive mass spectrometer (Thermo Scientific). Data analysis was performed using the ProLuCID and DTASelect2 implemented in the Integrated Proteomics pipeline IP2 (Integrated Proteomics Applications, Inc., San Diego, CA). Protein and peptide identifications were filtered using DTASelect and required a minimum of two unique peptides per protein and a peptide-level false-positive rate of less than 5%, as estimated by a decoy database strategy. Normalized spectral abundance factor (NSAF) values were calculated as described³³ and the data were analyzed using the Pathway Studio software^{34,35}.

Competitive growth rate assay. NcLiv Δ hpt (parental) and NcLiv_GRA15 or NcLiv_ROP16 transgenic parasites were mixed in 1:1 ratios and allowed to infect a confluent HFF monolayer. Resulting parasites that lysed out were used to infect new monolayers for IFA analysis and this process repeated for 5 passages. Cross-reactive toxoplasma polyclonal rabbit anti-ROP13 and polyclonal mouse anti-GRA14 was used to stain all parasites and mouse or rabbit anti-hemagglutinin (HA) (Invitrogen) was used to distinguish parental versus transgenic parasites and consequently to determine the replication rate of mutant strains *in vitro*.

Plaque Assay. For the plaque assay, 200 parasites per well were added in confluent HFFs and were incubated for 8 days at 37°C and 5% CO₂. The number of plaques was counted using the regular light microscope. The plaque size was measured using a Zeiss Axio Imager Z1 upright light microscope.

In vitro assays with host cells. To assess STAT3 phosphorylation during infection by *N. caninum*, parasites (MOI 10) were added to HFFs and infection was allowed to proceed for 18 h for detection of STAT3 by IFA and WB. Immunofluorescence and western blots were performed as described¹⁶ using antibodies specific for total STAT3 (Cell Signaling Technologies), Vimentin, RON5C or for the phosphorylated form of STAT3 (phospho-Tyr705) (Cell Signaling Technologies). Cytokine measurements were realized on bone marrow-derived macrophages (BMDMs) and splenocytes, infected with NcLiv Δ hpt, NcLiv_GRA15, or NcLiv_ROP16. After 24 h, culture supernatants were collected and stored at -70°C for cytokine quantification. IL-12p40 measurement was carried out by sandwich ELISAs according to manufacturer's instructions (BD Biosciences). Microplates were read in a plate reader (Molecular Devices, Sunnyvale, CA, USA) at 450 nm. Cytokine concentrations were calculated from standard curves of murine recombinant cytokines with detection limits of 2,000 to 31.3 pg/mL.

Statistical analysis. Statistical analysis was carried out using GraphPad Prism 6.0 (GraphPad Software Inc., La Jolla, CA, USA). Differences between groups were analyzed using ANOVA or Kruskal-Wallis test, when appropriate, with the respective Bonferroni or Dunn multiple comparison post-tests to examine all possible pairwise comparisons. The Kaplan–Meier method was applied to estimate the percentage of mice surviving at each time point after challenge and survival curves were compared using the Log-rank test. Values of P < 0.05 were considered statistically significant. Each experiment was independently conducted at least three times, and each condition was analyzed in triplicates.

References

1. Craeye, S. *et al.* *Toxoplasma gondii* and *Neospora caninum* in wildlife: Common parasites in Belgian foxes and Cervidae? *Vet Parasitol.* **178**, 64–69 (2011).
2. Goodswen, S. J., Barratt, J. L., Kennedy, P. J. & Ellis, J. T. Improving the gene structure annotation of the apicomplexan parasite *Neospora caninum* fulfils a vital requirement towards an in silico-derived vaccine. *Int J Parasitol* **45**, 305–318 (2015).
3. Yan, C., Liang, L. J., Zheng, K. Y. & Zhu, X. Q. Impact of environmental factors on the emergence, transmission and distribution of *Toxoplasma gondii*. *Parasit Vectors* **9**, 137 (2016).
4. Donahoe, S. L., Lindsay, S. A., Krocke, Berger, M., Phalen, D. & Šlapeta, J. A review of neosporosis and pathologic findings of *Neospora caninum* infection in wildlife. *Int J Parasitol* **4**, 216–238 (2015).
5. Li, W. *et al.* Identification and characterization of a microneme protein (NcMIC6). *Neospora caninum*. *Parasitol Res.* **114**, 2893–2902 (2015).
6. Montoya, J. G. & Liesenfeld, O. Toxoplasmosis. *Lancet.* **363**, 1965–1976 (2004).
7. Bradley, P. J. *et al.* Proteomic analysis of rhoptry organelles reveals many novel constituents for host-parasite interactions in *Toxoplasma gondii*. *Proc. Natl. Acad. Sci. USA* **102**, 34245–34258 (2005).
8. Dubreuil, J. F. Rhoptries are major players in *Toxoplasma gondii* invasion and host cell interaction. *Cell Microbiol.* **9**, 841–848 (2007).
9. Dlugonska, H. *Toxoplasma* rhoptries unique secretory organelles and source of promising vaccine proteins for immunoprevention of toxoplasmosis. *J. Biomed. Biotech* **2008**, 632424 (2008).
10. Howe, D. K. & Sibley, L. D. Development of molecular genetics for *Neospora caninum*: A complementary system to *Toxoplasma gondii*. *Methods.* **13**, 123–33 (1997).
11. Zhang, G. *et al.* Construction of *Neospora caninum* stably expressing TgSAG1 and evaluation of its protective effects against *Toxoplasma gondii* infection in mice. *Vaccine.* **28**, 7243–7247 (2010).
12. Hecker, Y. P. *et al.* Cell mediated immune responses in the placenta following challenge of vaccinated pregnant heifers with *Neospora caninum*. *Vet Parasitol.* **214**, 247–254 (2015).
13. Butcher, B. *et al.* *Toxoplasma gondii* rhoptry kinase ROP16 activates STAT3 and STAT6 resulting in cytokine inhibition and arginase-1-dependent growth control. *PLoS Pathog.* **9**, e1002236 (2011).
14. Yuan, Z. G. *et al.* Protective immunity induced by *Toxoplasma gondii* rhoptry protein 16 against toxoplasmosis in mice. *Clin and Vaccine Immunol* **18**, 119–124 (2011).
15. Jensen, K. D. *et al.* *Toxoplasma gondii* rhoptry 16 kinase promotes host resistance to oral infection and intestinal inflammation only in the context of the dense granule protein GRA15. *Infect Immun.* **81**, 2156–2167 (2013).
16. Rosowski, E. E. *et al.* Strain-specific activation of the NF-kappaB pathway by GRA15, a novel *Toxoplasma gondii* dense granule protein. *J Exp Med* **208**, 195–212 (2011).
17. Donald, R. G., Carter, D., Ullman, B. & Roos, D. S. Insertional tagging, cloning, and expression of the *Toxoplasma gondii* hypoxanthine-xanthine-guanine phosphoribosyltransferase gene. Use as a selectable marker for stable transformation. *J Biol Chem* **271**, 14010–14019 (1996).
18. Rome, M. E., Beck, J. R., Turetzky, J. M., Webster, P. & Bradley, P. J. Intervacuolar transport and unique topology of GRA14, a novel dense granule protein in *Toxoplasma gondii*. *Infect Immun.* **76**, 4865–4875 (2008).
19. Turetzky, J. M., Chu, D. K., Hajagos, B. E. & Bradley, P. J. Processing and secretion of ROP13: A unique *Toxoplasma* effector protein. *Int J Parasitol* **40**, 1037–44 (2010).
20. Nadipuram, S. M. *et al.* *In Vivo* Biotinylation of the *Toxoplasma* Parasitophorous Vacuole Reveals Novel Dense Granule Proteins Important for Parasite Growth and Pathogenesis. *mBio.* **7**, e00808–16 (2016).
21. Cardoso, M. R. *et al.* Adjuvant and immunostimulatory effects of a D-galactose-binding lectin from *Synadenium carinatum latex* (ScLL) in the mouse model of vaccination against neosporosis. *Vet Res.* **43**, 76 (2012).
22. Lei, T., Wang, H., Liu, J., Nan, H. & Liu, Q. ROP18 is a key factor responsible for virulence difference between *Toxoplasma gondii* and *Neospora caninum*. *PLoS One* **9**, e99744 (2014).

23. Marugán-Hernández, V., Ortega-Mora, L. M., Aguado-Martínez, A., Jiménez-Ruiz, E. & Alvarez-García, G. Transgenic *Neospora caninum* strains constitutively expressing the bradyzoite NcSAG4 protein proved to be safe and conferred significant levels of protection against vertical transmission when used as live vaccines in mice. *Vaccine*. **29**, 7867–7874 (2011).
24. Beckers, C. J., Wakefield, T. & Joiner, K. A. The expression of *Toxoplasma* proteins in *Neospora caninum* and the identification of a gene encoding a novel rhoptry protein. *Mol Biochem Parasitol* **89**, 209–23 (1997).
25. Pereira, L. M., Baroni, L. & Yatsuda, A. P. A transgenic *Neospora caninum* strain based on mutations of the dihydrofolate reductase-thymidylate synthase gene. *Exp Parasitol*. **138**, 40–47 (2014).
26. Pereira, L. M. & Yatsuda, A. P. The chloramphenicol acetyltransferase vector as a tool for stable tagging of *Neospora caninum*. *Mol Biochem Parasitol* **196**, 75–81 (2014).
27. Mota, C. M. *et al.* Fluorescent ester dye-based assays for the *in vitro* measurement of *Neospora caninum* proliferation. *Vet Parasitol*. **205**, 14–19 (2014).
28. Buxton, D., McAllister, M. M. & Dubey, J. P. The comparative pathogenesis of neosporosis. *Trends Parasitol*. **18**, 546–552 (2002).
29. Steinfeldt, T. *et al.* Phosphorylation of mouse immunity-related GTPase (IRG) resistance proteins is an evasion strategy for virulent *Toxoplasma gondii*. *PLoS Biology*. **8**, e1000576 (2010).
30. Carruthers, V. B. & Sibley, L. D. Sequential protein secretion from three distinct organelles of *Toxoplasma gondii* accompanies invasion of human fibroblasts. *Eur J Cell Biol* **73**, 114–23 (1997).
31. Yamamoto, M. *et al.* A single polymorphic amino acid on *Toxoplasma gondii* kinase ROP16 determines the direct and strain-specific activation of Stat3. *Exp Med* **206**, 2747–2760 (2009).
32. Virreira Winter, S. *et al.* Determinants of GBP recruitment to *Toxoplasma gondii* vacuoles and the parasitic factors that control it. *PLoS One*. **6**, e24434 (2011).
33. Chen, A. L. *et al.* Novel Components of the *Toxoplasma* Inner Membrane Complex Revealed by BioID. *MBio*. **6**, e02357–14 (2015).
34. Mota, C. M. *et al.* *Neospora caninum* activates p38 MAPK as an evasion mechanism against innate immunity. *Front. Microbiol* **7**, 1456 (2016).
35. Nikitin, A. Pathway studio the analysis and navigation of molecular networks. *Bioinformatics*. **19**, 2155–2157 (2003).

Acknowledgements

The authors thank to Marley Dantas Barbosa, Zilda Mendonça da Silva and Ana Cláudia Pajuaba for their technical assistance. This work was supported by Brazilian Funding Agencies (CNPq, FAPEMIG and CAPES).

Author Contributions

Conceived and designed the experiments: C.M.M., P.J.B., T.W.P.M. Performed the experiments: C.M.M., A.L.C., K.W., S.N. Analyzed data: C.M.M., P.J.B., T.W.P.M. Contributed reagents/materials/analysis tools and mice: P.J.B., T.W.P.M., J.A.W. Wrote the paper: C.M.M., T.W.P.M., P.J.B. All authors critically revised the manuscript.

Additional Information

Supplementary information accompanies this paper at doi:10.1038/s41598-017-03978-1

Competing Interests: The authors declare that they have no competing interests.

Publisher's note: Springer Nature remains neutral with regard to jurisdictional claims in published maps and institutional affiliations.



Open Access This article is licensed under a Creative Commons Attribution 4.0 International License, which permits use, sharing, adaptation, distribution and reproduction in any medium or format, as long as you give appropriate credit to the original author(s) and the source, provide a link to the Creative Commons license, and indicate if changes were made. The images or other third party material in this article are included in the article's Creative Commons license, unless indicated otherwise in a credit line to the material. If material is not included in the article's Creative Commons license and your intended use is not permitted by statutory regulation or exceeds the permitted use, you will need to obtain permission directly from the copyright holder. To view a copy of this license, visit <http://creativecommons.org/licenses/by/4.0/>.

© The Author(s) 2017